

Hornsea Project Three  
Offshore Wind Farm



## Hornsea Project Three Offshore Wind Farm

Appendix 33 to Deadline 7 submission – Le et al., 2014

Date: 14<sup>th</sup> March 2019

Document Control			
<b>Document Properties</b>			
Organisation	Ørsted Hornsea Project Three		
Author	Le et al., 2014		
Checked by	n/a		
Approved by	n/a		
Title	Appendix 33 to Deadline 7 submission – Le et al., 2014		
PINS Document Number	n/a		
<b>Version History</b>			
Date	Version	Status	Description / Changes
14/03/2019	A	Final	Submitted at Deadline 7 (14 <sup>th</sup> Mar 2019)

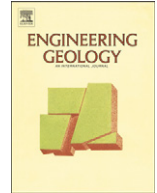
Ørsted

5 Howick Place,

London, SW1P 1WG

© Orsted Power (UK) Ltd, 2019. All rights reserved

Front cover picture: Kite surfer near a UK offshore wind farm © Ørsted Hornsea Project Three (UK) Ltd., 2019.



# Geological and geotechnical characterisation for offshore wind turbine foundations: A case study of the Sheringham Shoal wind farm



Thi Minh Hue Le <sup>a,\*</sup>, Gudmund Reidar Eiksund <sup>b</sup>, Pål Johannes Strøm <sup>c</sup>, Morten Saue <sup>d</sup>

<sup>a</sup> SINTEF Building and Infrastructure, SINTEF, Trondheim 7034, Norway

<sup>b</sup> Department of Civil and Transport Engineering, Norwegian University of Science and Technology (NTNU), Trondheim NO - 7491, Norway

<sup>c</sup> Statoil ASA, Martin Linges vei 33, 1364 Fornebu, Oslo, Norway

<sup>d</sup> NGL Inc., 2000 Dairy Ashford, Suite 322, Houston, TX, USA

## ARTICLE INFO

### Article history:

Received 19 August 2013

Received in revised form 23 January 2014

Accepted 8 May 2014

Available online 26 May 2014

### Keywords:

Foundations  
Offshore wind  
Sheringham Shoal  
Overconsolidated  
Clay  
Chalk

## ABSTRACT

This paper characterises the soil conditions at the Sheringham Shoal wind farm in the North Sea, in the context of designing foundations for offshore wind turbines. The purpose is to provide a realistic reference case study for research and practice in the emerging field of offshore wind energy. The soil data was obtained between 2005 and 2008 in an investigation program involving field measurements and laboratory experiments. The characterisation focuses on soil properties which are relevant for evaluating the performance of foundations for offshore wind turbines. The soil profile at the Sheringham Shoal site consists of four main units: two clay strata interbedded with a sand layer and underlain by a chalk bed. The heavily overconsolidated state of the clays and the densely compacted state of the sand dictate the behaviour of these soils. The chalk bed is characterised by varying degrees of weathering leading to significant variation in properties ranging from those typical for stiff soil to soft rock. These four main units, though differ considerably in soil composition, share several common characteristics including high shear strength and high stiffness but their shear stiffnesses reduce significantly both at high mobilised static shear strength and at medium to high mobilised strength under cyclic loading. The soil stiffness is an important input parameter for the design of offshore wind turbine foundations and hence the degradation of stiffness is an important issue at this wind farm. A number of soil properties at the site show considerable variability which requires a specific foundation design tailored for each location in order to be both safe and cost-effective.

© 2014 Elsevier B.V. All rights reserved.

## 1. Introduction

As a promising renewable energy source, offshore wind power is currently attracting strong interest from both academia and industry particularly in a number of European countries including Denmark, UK, Germany and Norway. If existing technology can be improved significantly to reduce the cost of energy produced by offshore wind to a competitive level, significant increase in the number of installations of turbines in the North Sea and the Baltic Sea can be expected over the next few decades. A key step to realize such a development is to understand the site conditions and the soil properties. In the North Sea, various sites and soil types have been characterised (e.g. Bjerrum, 1973; Andresen et al., 1979; Jardine et al., 1998; Long and Donohue, 2010). However, these studies are usually in connection with soil investigations to design foundations for oil and gas platforms. These types of foundations bear some important differences to those for offshore

wind turbines. Most notably, compared with the former, the latter is usually installed in larger number, in shallower water depth, subjected to lower vertical load but higher horizontal load and overturning moment (relative to the vertical load), and governed by dynamic response and fatigue rather than by ultimate limit states (ULS) (Houlsby et al., 2001; Byrne and Houlsby, 2006). Also, soil–structure interaction, cyclic behaviour and stiffness degradation characteristic are often strongly emphasized in the geotechnical characterisation for offshore wind turbine foundations. There are currently very few papers which present real soil properties in connection with offshore wind farms. These studies (e.g. Hamre et al., 2010; Firouzianbandpey et al., 2012) normally included the soil properties only as auxiliary information rather than as their main focus.

This paper presents a case study of the soil conditions at the Sheringham Shoal offshore wind farm (SSOWF) and discusses several aspects of the geological and geotechnical characterisation that are important for offshore wind turbine (OWT) foundations. The farm is located at ~20 m water depth and ~20 km north of the Norfolk coastline (the UK) in the North Sea (see top-right corner of Figure 1), with the total capacity of 317 MW from 88 wind turbines (Figure 1). Monopile

\* Corresponding author. Tel.: +47 93001834

E-mail addresses: [thi.le@sintef.no](mailto:thi.le@sintef.no) (T.M.H. Le), [gudmund.eiksund@ntnu.no](mailto:gudmund.eiksund@ntnu.no) (G.R. Eiksund), [pjst@statoil.no](mailto:pjst@statoil.no) (P.J. Strøm), [morten.saue@ngi-inc.com](mailto:morten.saue@ngi-inc.com) (M. Saue).

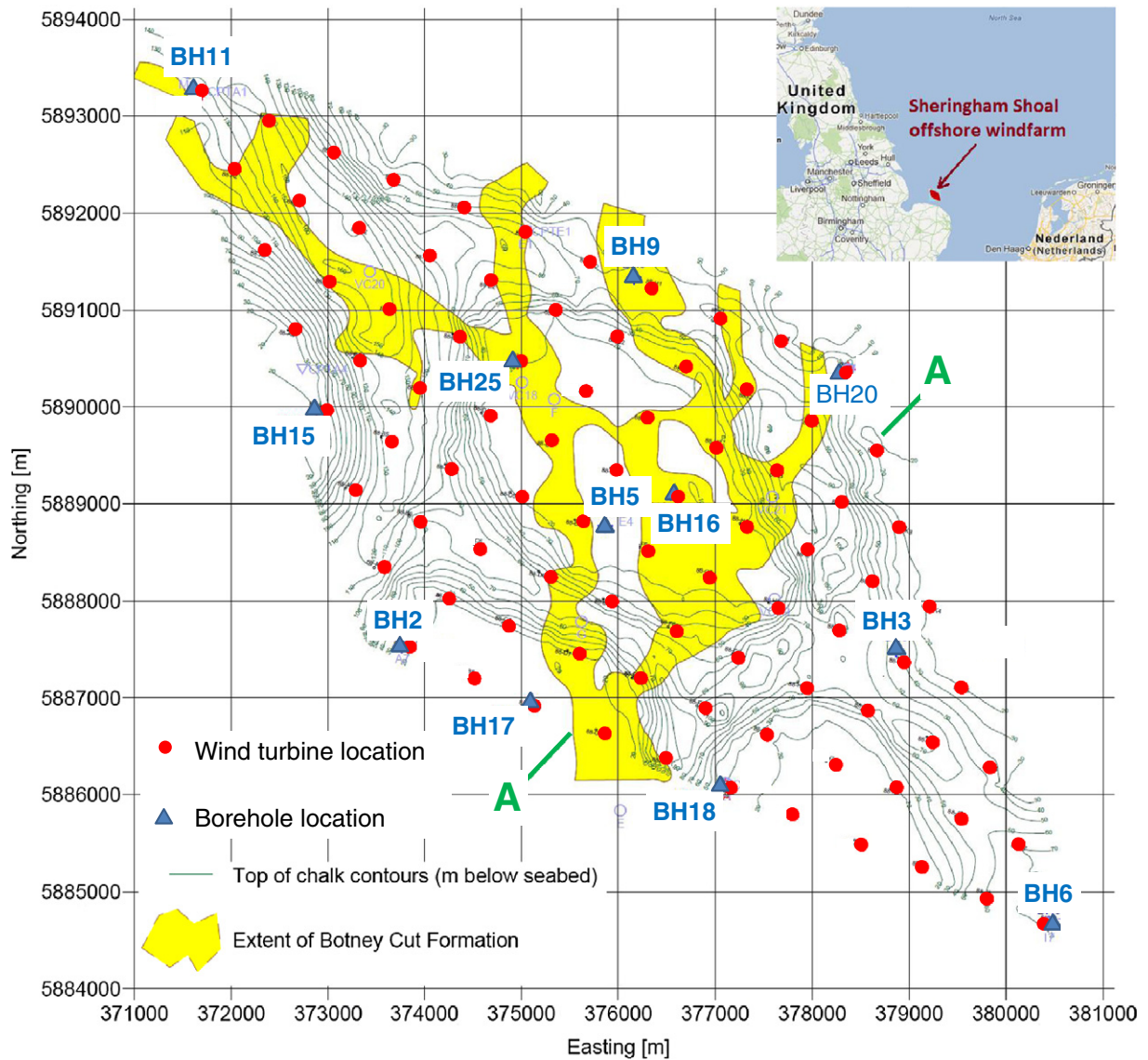


Fig. 1. Location of boreholes and wind turbines at the SSOWF.

foundations having diameters between 4.7 and 5.7 m and penetration depths between 23 and 37 m are used (Hamre et al., 2010). The field and laboratory data presented in this paper were obtained during a soil investigation program which involved a preliminary investigation in 2005–2006 followed by a main investigation in 2008. In this study, four main soil units found at the site are characterised which are, from the youngest to the oldest, the Bolders Bank (BDK) clay, the Egmond Ground (EG) sand, the Swarte Bank (SBK) clay and the Chalk (CK) rock. The characterisation focuses especially on properties that are relevant for the designing of OWT foundation including small strain stiffness, upper and lower bound strengths and stiffness degradation. The four soil units extend over large areas in the southern part of the North Sea (Cameron et al., 1992) and hence are likely to exist at other offshore wind farms in the vicinity. Indeed, clays of very similar characteristics to the BDK and SBK have been found at the planned Dogger Bank wind farm (T.I. Tjelta, (personal communication, 2012)). This study therefore aims to provide a source of reference for future geology/geotechnics practices and site investigation activities in this region. It also aims to contribute in guiding the young emerging offshore wind industry through the focused discussion of the implications of the geological and geotechnical characteristics of soils at the Sheringham Shoal site on the design of foundation. A section will be dedicated to

provide discussions and recommendations on the strategy to deal with soil variability, which will be useful for the practice of engineering geology in the North Sea region due to the highly variable soil condition at this region.

## 2. Geological condition and soil description

### 2.1. Geological condition

Geological records suggest that the SSOWF is situated in an area where Quaternary sediments are found directly on top of Cretaceous chalk (Cameron et al., 1992). The Quaternary period spans over the past 1.8 Ma during which ice sheets advanced and retreated many times across much of the high latitudes of the Northern hemisphere. The repeated glaciations resulted in overconsolidation or dense compaction of the main Quaternary soil units found at the SSOWF site due to the weight imposed by the ice sheets. In addition, the soil components of each soil unit tend to be a mix of various materials that were picked up by glacier during advancing and retreating, somewhat similar to components of till deposits occurring along the coastal areas of eastern England (Bell, 2002). Melt-water streams during glacial retreats left behind channels which caused rapid lateral changes in sediment

stratigraphy. Fig. 2 presents, as an example, the interpreted profile of cross-section A–A (indicated in Figure 1). The main soil units at the SSOWF site are identified based on data from the geological survey, borings, samplings and cone penetration tests (CPTs) (Birchall, 2012).

The seafloor is covered by a layer of shelly, fine to medium Holocene sand (HS) which varies in thickness from a few centimeters to 1–2 m. Underneath this sand, a relatively recent formation (~10–15 kyr ago), identified as the Botney Cut formation (BCT), occurs mainly as infills in subglacially produced melt-water channels with thickness varying from 0 to 5 m (Figures 1 and 2). This stratum consists of an upper glaciolacustrine and glaciomarine soft to firm silty clays (sometimes with pebbles and sand seams) and a basal part of a diamicton. Compared with other soil units (described subsequently), the HS and the BCT are relatively thin and hence unlikely to play a significant role in providing stiffness and strength for the foundations. In addition, data obtained for these soil layers are rather limited due to lack of good quality samples, resulting in highly variable measurements which bear large uncertainties. The BCT and the HS are therefore not characterised in detail in this study. These surface deposits can however be important in assessment of scouring at the SSOWF as they are prone to being eroded away by hydrodynamic processes activated by wind and wave actions. In assessing scour potential, locations covered with the HS should be differentiated from those with the BCT because scour holes can develop fast in sands with a few tidal cycles or a single storm event but can take months or years in clays. Near surface deposits can also be important in the evaluation of geohazards. This however is not a particular concern for the SSOWF because the site terrain is relatively flat (hence low risk of slope instability) and the area is not known to be at risk of seismic activity.

## 2.2. The Bolders Bank Formation (BDK)

The BDK unit represents the glacial advance during the last glacial period (~20 kyr ago) which appears as reddish to greyish brown stiff diamictons probably formed from subglacial and supraglacial sediments. It is described as a firm to stiff clay with pockets of sands and gravels and occasional boulders.

## 2.3. The Egmond Ground Formation (EG)

The EG unit was deposited in an open marine sedimentation environment following a sea level rise which inundated the North Sea after the decay of the Elsterian glaciation (~280–250 kyr). This formation is lithologically variable comprising of dense to very dense gravelly silty fine to medium sands interbedded with occasional stiff clay bands.

## 2.4. The Swarte Bank Formation (SBK)

The SBK unit was formed during the first glacial deposition in the region (~350–280 kyr) by filling a series of braided valleys cutting into the underlying chalk (Saue and Meyer, 2009). This formation consists of a basal till member occasionally interbedded with glaciofluvial dense sands or layers of gravels (Cameron et al., 1992). The gravel fraction is composed of fine to medium subrounded chalk. The main component is stratified glaciolacustrine hard silty clay which is sporadically overlaid by marine interglacial sediments. This formation has an undulating longitudinal profile and exhibits large variation in thickness (e.g. Figure 2).

## 2.5. Cretaceous Chalk (CK)

The bottom chalk, the oldest among the four soil units, was formed ~84–74 Ma ago (Saue and Meyer, 2009) and extends over a large area in the southern UK. The chalk in this region is divided into three members: the Lower, Middle and Upper Chalks. The Upper Chalk can be more than 200 m in thickness at the SSOWF site and, hence, is of interest to the current study. The chalk in this region appears to be more porous than chalks in other areas of the UK. This high porosity is conducive to the formation of “putty” chalk by weathering and freeze–thaw cycles which explains the presence of the weathered structureless materials grading downward into the intact chalk at the SSOWF site. The structureless upper chalk has thickness varying between 10 and 15 m and is composed of fine to coarse gravels mixed in a clayey sandy silty matrix. The structured lower intact chalk is a weak rock with low to medium density. This large variation in chalk weathering condition has also been observed in other areas in Norwich region (e.g. Smith and Rosenbaum, 1993). Using the chalk classification system suggested by Lord et al. (2002), the former is graded as Dm (i.e. structureless chalk with >35% comminuted chalk matrix) and Dc (i.e. structureless chalk with <35% comminuted chalk matrix) while the latter falls in B3 (i.e. intact chalk with typical discontinuity aperture <3 mm and typical discontinuity spacing between 60 and 200 mm) to B5 (i.e. intact chalk with typical discontinuity aperture <3 mm and typical discontinuity spacing <20 mm).

## 3. Investigation and testing program

The site investigation campaign was designed based on previous experiences at similar sites and/or for similar purposes (e.g. other offshore wind farms or offshore oil and gas facilities in the regions). The details of the campaign follow guidelines specified by certification bodies such as, for example, DNV No 30.4 (1992) and DNV-OS-J101 (2011).

The number of boreholes is recommended to be at least 10% of the number of turbine locations and a larger number might be required if the site condition is complex. At the SSOWF, 12 boreholes were drilled

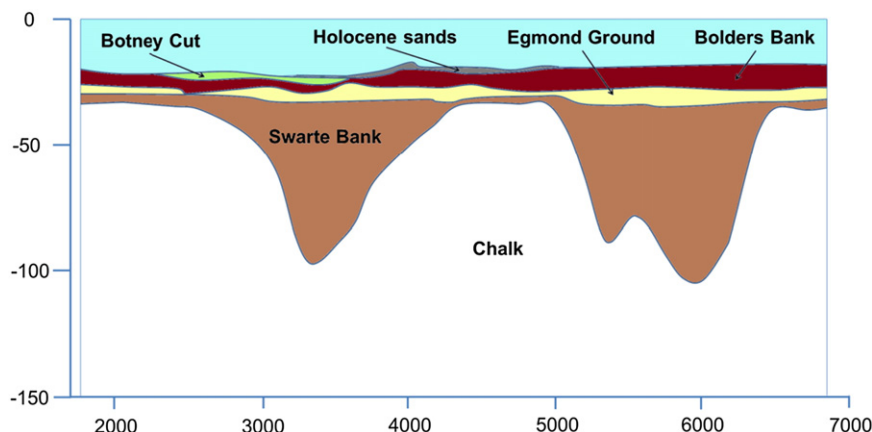


Fig. 2. Interpreted soil stratigraphy of a cross-section (A–A in Figure 1) of the SSOWF (unit in m).

including 5 during the preliminary investigation stage and 7 during the main investigation stage (more than 10% of the number of wind turbines). This number of borehole is considered necessary due to the relative complex soil condition at this site. The borehole locations were selected so that soil samples from all soil units (interpreted from the seismic survey and geological history) could be obtained and in sufficient quantity. In addition to borings at required locations (i.e. at all the corners and in the centre of the site), locations between the corners and between the corner and the centre were selected at relatively even distances (Figure 1). This strategy aims at gathering sufficient information for various purposes including: to update and verify the geological model from seismic survey and geological history, to balance the need for spatial information, and to take into account the large variability of soils at the SSOWF. The boreholes are approximately 4–5 km apart (Figure 1), which does reflect the main features in spatial variability of the field, as confirmed by information from CPTs and seismic survey. It is difficult to ascertain that all the spatial variability are captured by the spacing adopted, however extra boreholes are probably unnecessary for the purpose of designing the foundation considering the high cost involved. The number of boreholes and their spacing were, after the investigation campaign, found to be sufficient to verify the geological model interpreted from seismic survey and geological history. They also provided adequate amounts of soil materials from different units for laboratory testing.

Since monopiles were identified as a possible foundation option at the SSOWF based on the initial soil investigation, the borehole depths for the main soil investigation were tailored to suit this foundation type. The borehole depth is half to one pile diameter (i.e.  $\approx 3$ –10 m) below the pile tips (DNV-OS-J101, 2011). The depth was also designed to be sufficient so that samples from all units can be taken. The boreholes at the SSOWF vary from 26 to 70 m in depth depending on location.

Although much experience of designing the soil investigation program for the wind industry has been derived from the oil and gas industry, there are some clear differences between the soil investigation programs between the two industries. Foundations for oil and gas facilities can vary significantly in sizes and, hence, their soil investigation programs also vary significantly in extent, concentration and methods selected. A jack-up platform, for example, tends to cover a relatively small area (e.g. 50 m  $\times$  50 m) which requires a soil investigation campaign spreading over much smaller area than an offshore wind farm such as the SSOWF. Conversely, a large floating platform can involve soil investigation over an area as large as a wind farm, but much less concentrated effort (i.e. normally the investigation will only require 1 CPT and 2 boreholes at each template or, for anchored platforms, one CPT at each anchor location and a borehole for each anchor cluster). The relevant depth of boring is relatively similar between foundations for oil facilities and for offshore wind farms.

At the SSOWF, the field investigation included measurements of small strain stiffness ( $G_{max}$ ) at four boreholes, and numerous CPT measurements of cone resistance ( $q_c$ ) (which were used to estimate undrained shear strength ( $s_u$ ) of clays and relative density ( $D_r$ ) of sands). The boreholes were advanced from the mudline by GEOPOR rotary drilling. Push sampling and CPT measurements were performed from the mudline until encountering the chalk. Push sampling was then continued into the chalk until the end of the boreholes. The  $G_{max}$  was obtained by the suspension PS velocity logging method (GeoVision, 1994).

Samples were collected at each borehole by Shelby tubes and core samplers for advanced testing in offshore and onshore laboratories. The offshore laboratory tests consisted of soil description and classification tests (for water content ( $w$ ), plastic (PL) and liquid (LL) limits, plasticity ( $I_p$ ) and liquidity ( $I_L$ ) indices); index shear strength testing and unconsolidated undrained (UU) triaxial tests. In onshore laboratories (at the Norwegian Geotechnical Institute – NGI), a testing program was conducted including: classification tests (for  $w$ ,  $I_p$ ,  $I_L$ ), total and dry unit weights ( $\gamma$ ,  $\gamma_{dry}$ ), fines and clay contents, remoulded shear

strength ( $s_{u,rem}$ ) and sensitivity ( $S_t$ ); constant rate strain (CRS) oedometer tests for vertical coefficient of consolidation ( $c_v$ ) and constant head test for permeability ( $k$ ); bender element (BE) tests for  $G_{max}$ ; shear box and interface shear box tests for peak and residual shear strength ( $\tau_{peak}$  and  $\tau_{res}$ ); ring shear tests for residual friction angle ( $\phi_r$ ); direct simple shear (DSS), compression and extension undrained triaxial tests for undrained shear strength ( $s_u^{DSS}$ ,  $s_u^C$  and  $s_u^E$ ); and drained triaxial tests for friction angle ( $\phi'$ ). In particular, cyclic tests were conducted in both DSS and triaxial apparatuses from which the degradation of stiffness with cyclic loading of the four main soil units is investigated shedding light on one of the most important aspects governing the design of OWT foundations.

The characterisation of the BDK, EG, SBK and CK presented in this paper is based on both field measurements and onshore/offshore laboratory tests. The ranges of the basic soil properties are summarized in Table 1 while Fig. 3 shows an example of soil profile (at borehole BH3).

## 4. Index soil properties

### 4.1. Water content ( $w$ ), total and dry unit weight ( $\gamma$ , $\gamma_{dry}$ ) and relative density ( $D_r$ )

The measurements included in Figs. 3 and 4 suggest that there is no apparent decrease of  $w$  with depth at the SSOWF (as usually observed for normally consolidated soils). Both the BDK and the SBK exhibit relatively low  $w$  for clays (average at  $\sim 17$  and 16%, respectively), which indicates stiff behaviour and overconsolidated state similar to the  $w$  observed for various British overconsolidated clays (e.g. see Cripps and Taylor, 1987). The average  $w$  of the SBK increases to around 25% from 40 m downward, consistent with the increases in fines and clay contents (Table 1). Considerable variation is observed for the  $w$  of the EG due to the lithological non-uniformity of this sand unit (Figure 4). The  $w$  of the CK is relatively high (averaging at  $\sim 28\%$ ) due to high porosity which implies potentially high brittleness during installation and hence low side friction for pile foundation.

For all four soil units, the values of  $\gamma$  and  $\gamma_{dry}$  estimated using correlations with  $w$  (assuming a saturated state and constant specific gravity  $\sim 2.65$ ) are consistent with their corresponding values estimated from advanced tests in onshore laboratory and from measuring dimension and weight of waxed samples in offshore laboratory. The range of mean values of  $\gamma$  is from  $\sim 17$ –21.3 kN/m<sup>3</sup>. The  $\gamma_{dry}$  is of particular interest for chalk because it is often used as an index parameter in correlation with other soil properties. The average value of  $\gamma_{dry}$  of the CK is  $\sim 15.2$  kN/m<sup>3</sup> which falls in the low end of the medium dry density range for chalk (15.2–16.7 kN/m<sup>3</sup>) suggested by Bell et al. (1999) and Lord et al. (2002).

The  $D_r$  for the EG sand is interpreted from CPT cone resistance using the relationship suggested by Baldi et al. (1986) and a unity coefficient of earth pressure at rest ( $K_0 = 1$ ). Note that the value of  $K_0$  tends to decrease with depth, however the thickness of the EG unit is generally less than 7 m at this site and hence the assumption of a constant  $K_0$  is considered to be acceptable. The value of  $D_r$  varies over a wide range ( $\sim 30$ –85%) with an average at  $\sim 70\%$  which indicates densely compacted sand (e.g. Figure 3).

### 4.2. Grain size composition and plasticity indexes

The grain size distributions at various depths for the EG, SBK and CK vary significantly even within a single soil unit (e.g. Figure 5), which reflects the variable composition of these glacial deposits. The fines content (particles < 0.063 mm) and the clay content (particles < 0.002 mm) of different samples scatter over wide ranges for both the BDK and the SBK. The fines content of these soils can be as high as 98% in some samples, but also drops to as low as 5% if sand lenses are encountered during sampling. The SBK has on average higher fines content than the BDK

**Table 1**  
Average ranges of the main soil properties.

	BDK	EG	SBK	CK
Depth (m)	0–12	7–18	15–40	40–62
Geological age	Pleistocene	Pleistocene	Pleistocene	Campanian
Description	Stiff clay	Dense sand	Very stiff clay	Weak rock
w (%)	10–24	18–28	10–22	15–33
$I_p$ (%)	14–20		10–20	20–30
$I_L$	–0.1–0.3		–0.4–0.6	0.3–1.5
$\gamma$ (kN/m <sup>3</sup> )	19.7–22.5	19.1–20.8	20.0–22.5	18.4–21.4
Fines content (%)	52–62	2	83–97	95–98
Clay content (%)	24–36		32–48	12–60
$s_{u,rem}$ (kPa)	40–150 <sup>a</sup>		60–400 <sup>a</sup>	
$S_t$	1–2		2–3.5	
OCR	4–40 <sup>b</sup>		3–30 <sup>b</sup>	
$D_r$ (%)		40–120		
$c_v$ (m <sup>2</sup> /s)	1.0–2.0 ( $\times 10^{-7}$ )	2.8 ( $\times 10^{-1}$ )	7.5–7.8 ( $\times 10^{-6}$ )	1.0–4.0 ( $\times 10^{-4}$ )
k (m/s)	1.8–2.0 ( $\times 10^{-10}$ )	3.2 ( $\times 10^{-5}$ )	2.0 ( $\times 10^{-9}$ )	1.5–5.7 ( $\times 10^{-8}$ )
$G_{max}$ (MPa)	10–150 <sup>c</sup>	16–280 <sup>c</sup>	140–1000 <sup>c</sup>	100–2500 <sup>c</sup>
$s_u$ (kPa)	20–250 <sup>a</sup>		180–1600 <sup>a</sup>	100–1400 <sup>c</sup>
$s_{u,rem}^{DSS}/s_u^C$	0.75		0.43	0.74
$s_{u,rem}^E/s_u^C$	0.67		0.48	0.67
$\phi'$ (°) <sup>d</sup>	40.5 <sup>e</sup> , 36.0 <sup>f</sup>	44.0, 47.5–49.5 <sup>g</sup>	31.0–33.5	33.5–41.0, 37.0 <sup>g</sup>
$\phi_r'$ (°) <sup>h</sup>			25	30
$\tau_{res}/\tau_{peak}^i$			0.30–0.84	0.82–0.98
$\tau_{res}/\tau_{peak}^j$			0.64–0.98	0.80–1.00

- <sup>a</sup> Varies with depth
- <sup>b</sup> Decreases with depth
- <sup>c</sup> Increases with depth
- <sup>d</sup> From undrained triaxial tests unless specified
- <sup>e</sup> 0–5 m
- <sup>f</sup> 5–12 m
- <sup>g</sup> From drained triaxial tests
- <sup>h</sup> Ring shear and shear box tests
- <sup>i</sup> Shear box tests
- <sup>j</sup> Interface shear box tests

(Table 1). The clay content varies at 10 – 50% for the BDK and 10–70% for the SBK.

The soil plasticity index ( $I_p$ ) has been shown to be positively correlated with the rate of stiffness degradation and negatively correlated with the damping ratio (Vucetic and Dobry, 1991), and hence can have important implications on the performance of OWT foundations.

Both the BDK and the SBK exhibit low to medium plasticity (e.g. Figure 3 and Table 1) which might be explained by the effect of “rock flour” associated with their glaciation origin as observed for the Drammen clay (Tanaka et al., 2001). The CK also shows low plasticity (~8%) which falls toward the lower limit of the typical  $I_p$  range for chalk (4–40%) reported by Lord et al. (2002). The liquidity index ( $I_L$ ) for

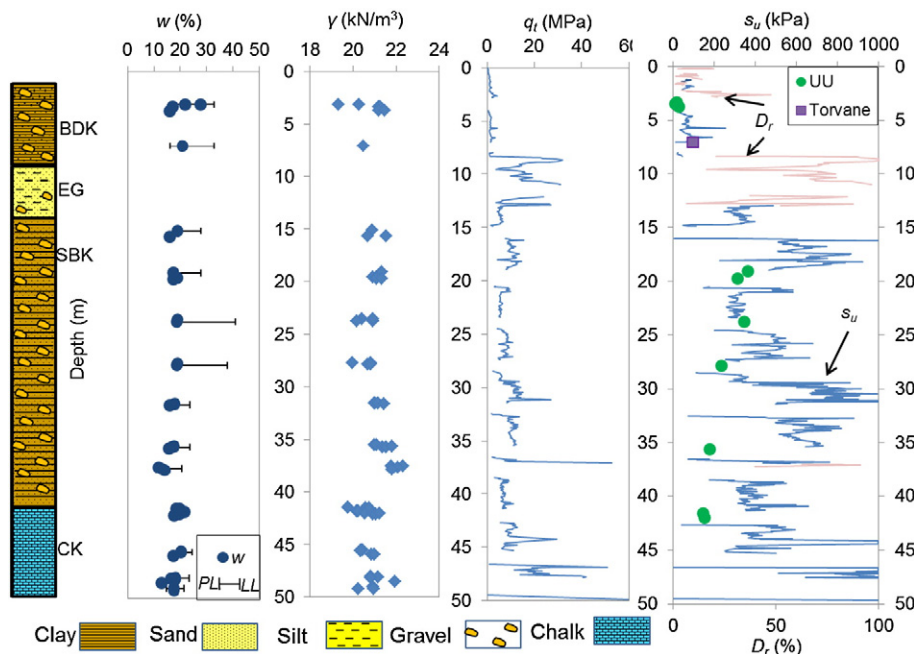


Fig. 3. Example of a typical boring profile and corresponding soil properties (BH3).

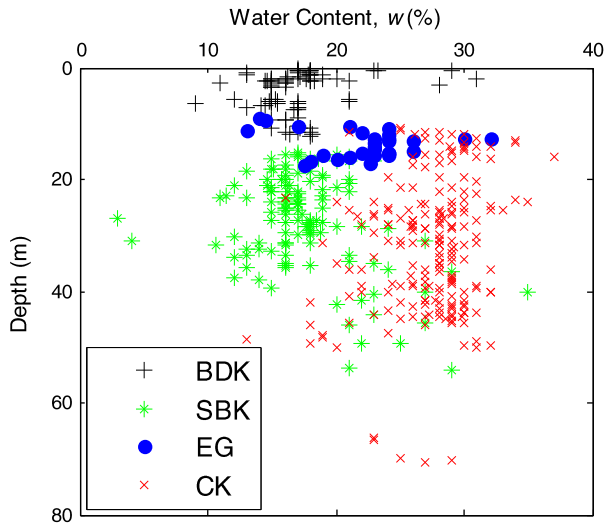


Fig. 4. Variation of water content (*w*) with depth of the four main soil units.

the BDK and the SBK drops to negative values in a number of samples (Table 1) indicating stiff to very stiff behaviour in the field.

### 5. Deformation characteristics

#### 5.1. Coefficient of consolidation (*c<sub>v</sub>*) and permeability (*k*)

Permeability of the four soil units is investigated by constant head test, while the coefficient of consolidation is derived from oedometer test at around the effective overburden pressure. Both the values of *c<sub>v</sub>* and *k* differ significantly between different soil units but vary only slightly with depth within each unit (Figure 6). The rates of consolidation (inferred from the corresponding values of *c<sub>v</sub>*) is lower for the BDK than for the SBK, CK and EG. This is consistent to the fact that the BDK is considerably less permeable than the SBK, CK and EG. Except for the EG which is a sand and hence has relatively high permeability ( $k > 10^{-5}$  m/s), the other three units have relatively low permeability ( $10^{-7} > k > 10^{-10}$  m/s), which falls in the typical permeability range for clays and chalk. These low permeability soil strata are susceptible to accumulation of excess pore water pressure. This can be particularly problematic during cyclic loading, especially for large diameter piles embedded in poor drainage condition and subjected to large number of load cycles. The sand lenses interbedded in the BDK and the SBK at the SSOWF site might however act as ‘drains’ which would alleviate the accumulation of excess pore water pressure during loading.

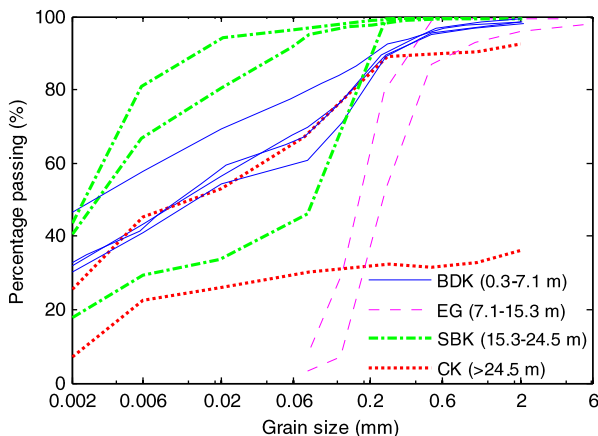


Fig. 5. Grain size distribution at various depths from a representative borehole (BH15).

#### 5.2. In situ stress condition and over consolidation ratio (OCR)

The OCR at a certain depth is defined as the ratio between the pre-consolidation stress ( $\sigma'_c$ ) and the vertical effective stress ( $\sigma'_v$ ) at that depth (i.e.  $OCR = \sigma'_c / \sigma'_v$ ). The value of OCR can be estimated directly from evaluating  $\sigma'_c$  and  $\sigma'_v$ ; or indirectly from correlations with other soil parameters, for example, those measured by the CPT or in triaxial tests. Fig. 7 compares the OCR values estimated by various methods.

The value of  $\sigma'_v$  can be estimated from the total unit weight while the value of  $\sigma'_c$  can be interpreted from laboratory tests or by considering the geological history of the site. The geological history of the SSOWF is governed by repeated glaciations and possible periods with permafrost. The value of  $\sigma'_c$  can be approximated assuming an equivalent surface stress from 25 to 75 m of ice for the BDK and 130–550 m of ice for the SBK (Siegerta and Dowdeswell, 2004). This method results in a decreasing profile of OCR with depth which is relatively consistent with estimations of OCR using the values of  $\sigma'_c$  measured in CRS oedometer (OE) (for the BDK) (Figure 7a).

Fig. 7 also shows the upper and lower limits of the range of OCR interpreted from the normalised cone resistance ( $Q_f$ ) by employing the following empirical correlation (Lunne et al., 1997):

$$OCR = k_{OCR} \cdot Q_f \quad (1)$$

A correlation factor  $k_{OCR} = 0.3$  is used as it normally offers reasonable consistency between the field and the laboratory tests (Saeue and Meyer, 2009). Indeed, Fig. 7 shows that the ranges of OCR from the CPTs for both the BDK and the SBK agree relatively well with the values of OCR interpreted from anisotropically consolidated undrained triaxial (CAU) compression tests, using an empirical correlation between  $s_u/\sigma'_v$ , OCR and  $I_p$  suggested in Lunne et al. (1997).

The BDK is highly overconsolidated in the top layer (OCR ~15–50 in the first 2 m), then its OCR decreases to <10 below 7 m. The value of OCR for the SBK ranges between 4 and 20 but its upper bound exhibits a value of 40–50 at certain depths (Figure 7b). This is possibly associated with sand layers, which means that the interpretation of OCR from Eq. (1) is not applicable.

At a similar depth, the OCR for the BDK and SBK are from slightly to considerably higher than that of several well-characterised clays in Northern Europe reported in the literature, for example, London clay ~4–16 at 7–50 m depth (Gasparre, 2005), Troll clay ~1.5 at 0–75 m depth (Lunne et al., 2006) and Dublin Bolder clay <4 at 0–24 m depth (Long and Menkiti, 2007). These values of OCR are comparable to that of glacial clays in nearby vicinity such as at Cowden site (UK) ~2–50 at 3–11 m depth (Lehane and Jardine, 1994). The large OCRs have several implications for the design and performance of wind turbine foundations at the SSOWF. First, soil parameters for preliminary design are, in practice, sometimes estimated using correlations between the OCR with other soil properties, for example with  $s_u$  (Wroth, 1984; Ladd, 1991) or with  $K_o$  (Mayne and Kulhawy, 1982). However, the verification of these correlations is based mainly on soil data having OCR <10 with limited samples having OCR >10. Therefore, these correlations, if needed, should be applied with extreme caution to heavily overconsolidated soils such as the BDK or SBK.

In addition, the OCR can considerably influence soil initial stiffness in both lateral and axial loading conditions through the initial slopes of the p–y and t–z curves respectively (if employing these curves for serviceability limit state (SLS) or fatigue analysis of wind turbine foundations (DNV, 2011)). For example, unless data indicate otherwise, the initial slope ( $k_{py}$ ) of p–y curve for clay is suggested to be calculated from the ultimate lateral resistance ( $p_u$ ), pile diameter (*D*) and vertical strain at a certain stress ( $\epsilon_c$ ) (DNV, 2011) as follows:

$$k_{py} = \xi \cdot p_u / (D \cdot \epsilon_c^{0.25}) \quad (2)$$

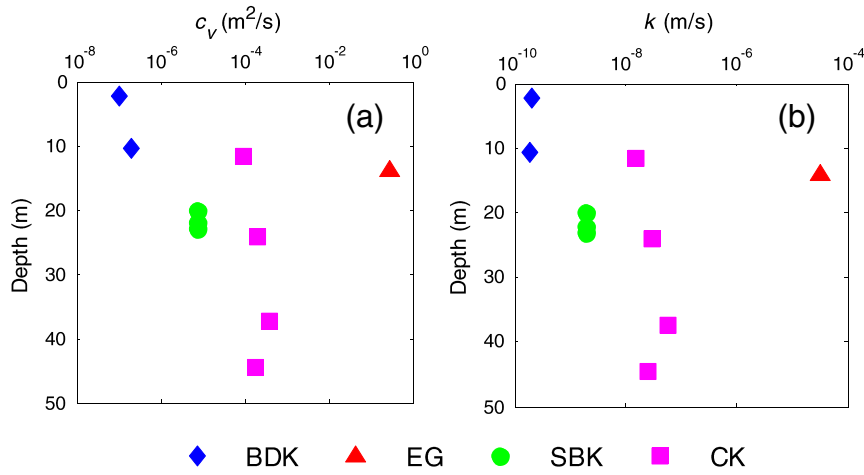


Fig. 6. Variation of (a) consolidation coefficient ( $c_v$ ) and (b) permeability ( $k$ ) with depth.

In Eq. (2), the empirical coefficient  $\xi$  is recommended to be 10 for normally consolidated clays but three times higher ( $\xi = 30$ ) for overconsolidated clays.

Similarly, the initial slope of  $t$ - $z$  curve is also positively correlated with the OCR. For example, the initial shear modulus  $G_o$  for axial loading is suggested by (Eide and Andersen, 1984) to correlate with the OCR as follows:

$$G_o = 600 \cdot s_u - 170 \cdot s_u \cdot (\text{OCR} - 1)^{0.5} \quad (3)$$

Both Eqs. (2) and (3) imply that the BDK and SBK will behave very stiff at very small initial strain due to their high OCR which will contribute to, for example, high natural frequencies of the wind turbine tower. High initial stiffnesses also imply a risk of significant degradation of stiffness with loading, as will be discussed in detail in later sections.

### 5.3. Small strain shear modulus ( $G_{max}$ )

A key soil parameter for evaluating the foundation performance in fatigue and serviceability limit state is the shear modulus ( $G$ ). The shear modulus at very small strain  $G_{max}$  is a fundamental soil property which can be applied to static, dynamic, drained and undrained conditions. This is because, at the onset of loading in the field, soil has not yet “determined” the path that it is going to follow. This path depends on, among other factors, loading rate and permeability (Mayne, 2006). The  $G_{max}$  is particularly an important soil parameter for OWT because it directly influences the eigenfrequency. Also, this parameter can be used directly to estimate the foundation stiffness at low to moderate load amplitude which is relevant for fatigue life evaluation.

At the SSOWF site, the values of  $G_{max}$  were measured at 4 boreholes (15, 16, 17 and 20 in Figure 1) using the PS suspension logging method, and cross-checked with those measured by BE in DSS and TXL specimens. During PS suspension logging, the shear wave velocity ( $v_s$ ) was

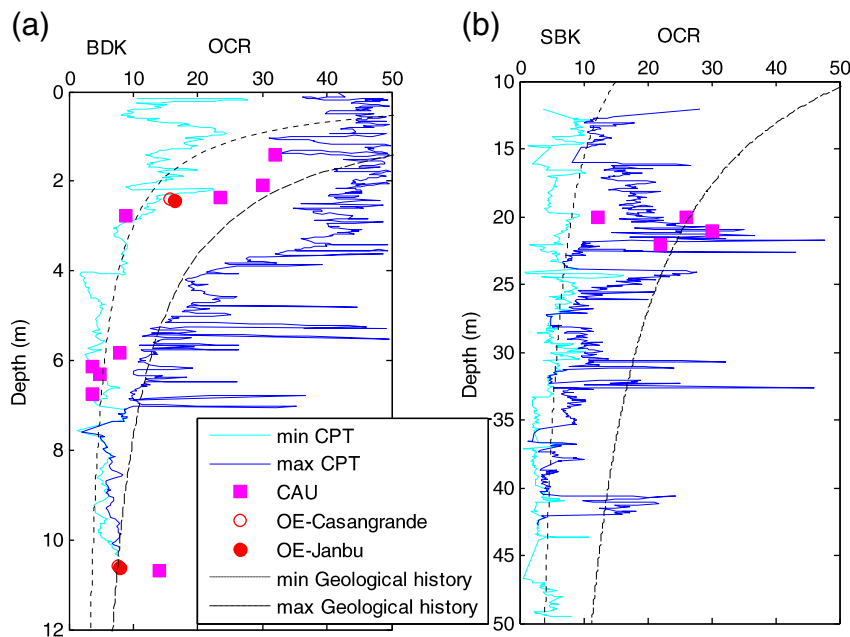


Fig. 7. Overconsolidation ratio (OCR) for the BDK and SBK clays.

determined at a nominal 1 m interval by the PS logger down to 45 m depth below the seabed. The  $G_{max}$  was then calculated from  $v_s$  and the soil bulk density ( $\rho$ ) ( $G_{max} = \rho v_s^2$ ). The values of  $G_{max}$  estimated at different boreholes span relatively similar variation ranges and hence are not differentiated in Fig. 8. Note that the  $G_{max}$  discussed subsequently is average value and any stiffness anisotropy at the site has not been considered.

The  $G_{max}$  exhibits an overall increasing tendency with depth which is especially visible for the SBK and the CK due to the large thicknesses of these units (Figure 8). This increase is likely to be associated with the increasing geologic age and the increasing overburden pressure with depth (Vucetic and Dobry, 1991). All four soil units behave stiff to very stiff in the small strain region corresponding to significantly large values of  $G_{max}$ . In particular, the range of  $G_{max}$  for the BDK is ~10–30 MPa near the surface and ~150 MPa at 10 m depth, which is rather typical for low plasticity overconsolidated clays. For example, London clay (with OCR ~4–16) has a range of  $G_{max}$  of ~10–30 MPa near the surface and increasing to ~100 MPa at 10 m depth (Cripps and Taylor, 1986; Gasparre, 2005; Clayton, 2011). The  $G_{max}$  of the EG sand varies over a range of 15–280 MPa. The high ‘upper bound’ is consistent with the high  $D_r$  of this dense sand. The SBK shows very large  $G_{max}$  varying from 150 MPa (at 15 m depth) to 1000 MPa (at 30 m depth) which is comparable to other stiff overconsolidated clays such as the Dublin Boulder Clay ( $G_{max}$  ~200 MPa at depth <4 m and  $G_{max}$  ~1500 MPa at 30 m depth) (Long and Menkiti, 2007). The  $G_{max}$  for chalk ranges from 100 MPa (at 12 m depth) to 2000–2500 MPa (at 30–40 m depth) with several very large measurements of almost 5000 MPa at 45 m (not included in Figure 8). These very large  $G_{max}$  values have also been observed, for example, for chalks found in the Fehmarn Belt Fixed link project between Denmark and Germany ( $G_{max}$  ~ 6000 MPa) (Rambøll, 2011).

Fig. 8 also shows that the values of  $G_{max}$  obtained in the BE tests tend to be smaller than that obtained by the PS logger (with the exception of the BDK unit). This underestimation of the field measurements by the laboratory data is likely to be the result of disturbances caused by the sampling process. These disturbances ‘loosen’ overconsolidated soil samples and hence decrease soil stiffness (Elhakim, 2005). Similar discrepancy between the values of  $G_{max}$  measured in the laboratory and at the field has also been observed for other overconsolidated soils, for example, the Dubai gypsiferous mudrock or London Eocene sandy clay (see Clayton (2011)).

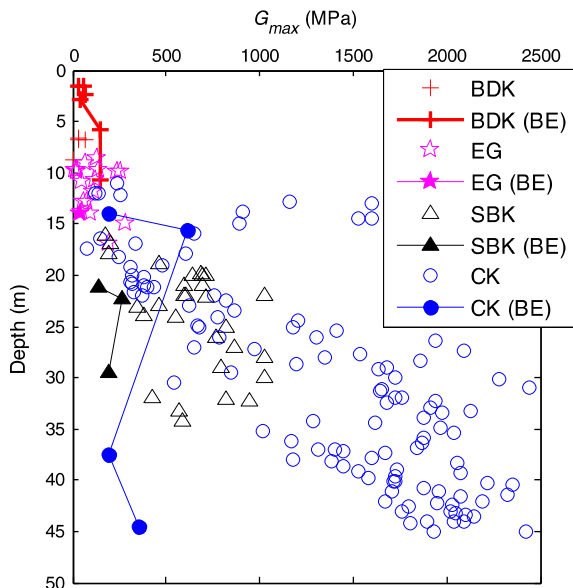


Fig. 8. Variation of small strain stiffness ( $G_{max}$ ) with depth.

## 6. Shear strength

### 6.1. Undrained shear strength ( $s_u$ )

For OWT, the foundation dimension is determined by the lower bound while the installation capacity is governed by the upper bound of the  $s_u$ . Due to the strong link between stiffness and strength, the range between the lower and the upper bound is also important for stiffness evaluation. Therefore, the  $s_u$  and its bound values are important parameters for the designing of OWT foundation.

The  $s_u$  was investigated in the field using downhole CPT, while good quality samples retrieved from the boreholes were tested in the laboratory mainly in anisotropically consolidated undrained compression and extension (CAUC and CAUE) triaxial tests and unconsolidated undrained triaxial (UU) tests. The  $s_u$  is related to the corrected cone resistance ( $q_t$ ) measured by the CPTs, the total vertical stress ( $\sigma_v$ ) and the cone factor ( $N_{kt}$ ) as follows:

$$s_u = (q_t - \sigma_v) / N_{kt} \tag{4}$$

Using  $N_{kt} = 15$  (for the BDK and SBK) and  $N_{kt} = 20$  (for the CK), relatively consistent patterns of variation can be seen between the field and the laboratory results. However, the values of  $s_u$  obtained in the laboratory tend to fall in the lower ends of the ranges indicated by the CPT (Figure 9).

The  $s_u$  varies quite significantly with depth and in lateral direction (i.e. between different boreholes). In particular, the value of  $s_u$  for the BDK ranges between ~50 and 500 kPa down to 7 m, then the variation range decreases between 7 and 11 m (Figure 9a). The narrower variation should however be treated with caution in this case because only three laboratory tests and two CPTs are available at depth below 7 m. The value of  $s_u$  for the SBK varies from 200 to 800 kPa with several prominent peaks (Figure 9b). For the CK, the range of  $s_u$  is ~100–600 kPa between 16 and 21 m (based on limited data) which is narrower than the approximate range of 200–1500 kPa from 21 m downward. This trend might be associated with the weathered and structureless state of chalk at shallower depth leading to a reduction in  $s_u$  compared with the intact deeper chalk. The values of  $s_u$  for the BDK and the SBK are rather typical for stiff to very stiff heavily overconsolidated clays while that for the CK is consistent with the shear strength range observed for weak rocks. The prominent peaks observed for the CPT data are likely to be caused by coarse-grained soil lenses dominated by sands or gravels in the BDK and the SBK units, or with harder layers in the CK unit. The measurement of  $s_u$  for CK should be interpreted with caution as some readings might be erroneous due to the existence of gaps within the brittle chalk mass.

### 6.2. Effective stress parameters

The effective stress parameters (i.e. friction angle  $\phi'$  and cohesion  $c'$ ) are derived, in the current study, mainly from the effective stress paths of triaxial undrained tests (CAUC and CAUE) and complimented with a few drained tests (CADC and CADE) conducted for the EG and the CK. For all four soil units, the effective stress paths shown in Fig. 10 indicate dilatant behaviour which is consistent with their high OCR values (for clays and chalk) and high  $D_r$  (for sand). The effective stress parameters are most relevant for the EG unit as they are used for both construction of p–y curves and for driveability evaluations but are also relevant for other soil units to model their long-term behaviour.

The values of peak  $\phi'$  are relatively high for all four soil units, and are the same or close between compression and extension conditions (Figure 10). Note that the mean effective stress in Fig. 10 is the average of effective stresses in various directions. In case of triaxial tests, this is equal to one-third of the sum of two times the radial effective stress plus the vertical effective stress. The BDK shows slightly higher  $\phi'$  at depth range from 0 to 5 m (~40.5°) than at larger depth from 5 to

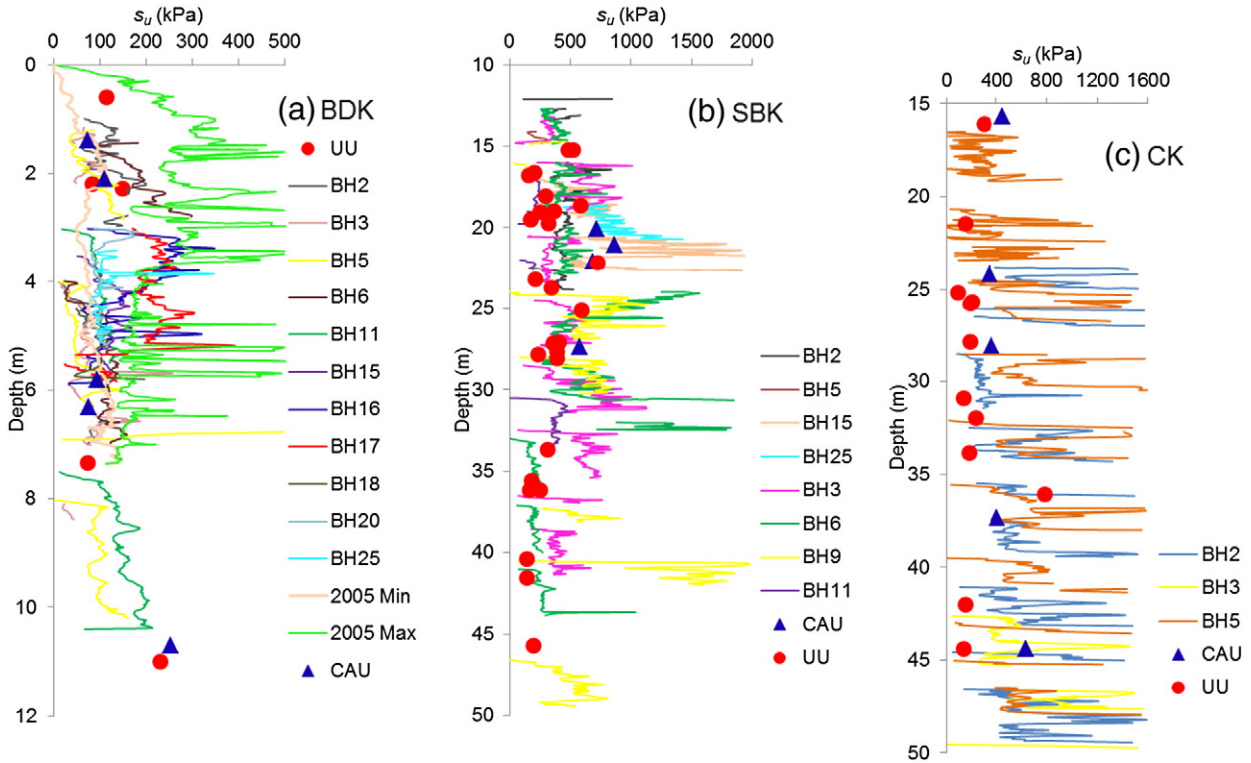


Fig. 9. Undrained shear strength ( $s_u$ ) of the BDK, SBK and CK. Note that the curves “2005 Min and 2005 Max” indicate the lower and upper bounds respectively of CPT measurements from a related investigation by Fugro conducted in 2005.

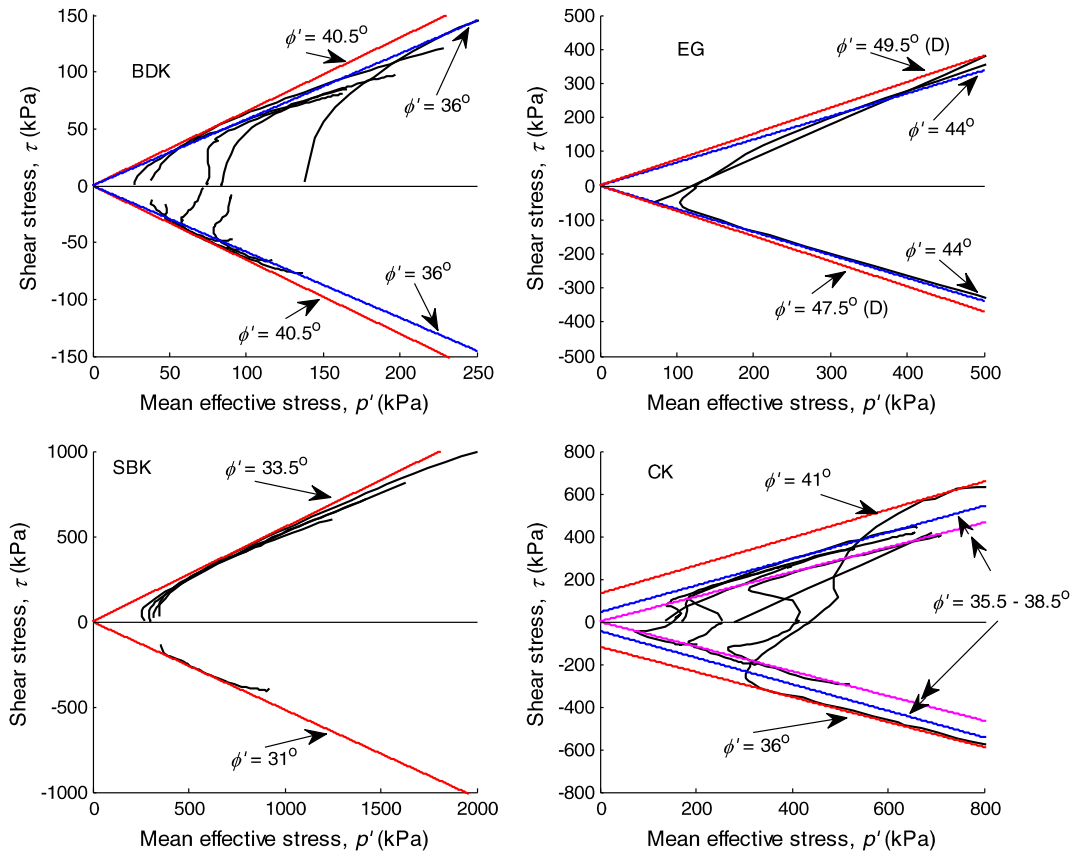


Fig. 10. Effective stress paths from compression and extension triaxial tests and corresponding friction angles ( $\phi'$ ). Positive direction for compression and negative direction for extension tests.

12 m (~36.0°) which implies the dependency of  $\phi'$  on stress level. The loading condition also plays a role in determining the value of  $\phi'$  as the EG has  $\phi' \approx 44.0^\circ$  estimated from the undrained tests but slightly higher values from drained tests (47.5–49.5°). The SBK shows lower values of  $\phi'$  than the BDK and EG, and lower for the active state ~31.0° (extension) than passive state ~33.5° (compression). The values of  $c'$  are zero for these three soil units. The weathered structureless CK(Dc) exhibits values of  $\phi'$  varying from 35.5° (with  $c' = 0$  kPa) to 38.5° (with  $c' = 40$  kPa), smaller than  $\phi' = 41.0^\circ$  (with  $c' = 131$  kPa) for the intact structured CK(B3).

6.3. Remoulded shear strength ( $s_{u,rem}$ ) and sensitivity ( $S_t$ )

The  $s_{u,rem}$  is an intrinsic soil property which is required for evaluating the skin friction for skirt penetration resistance and pile drivability or for axial pile capacity analysis by, for example, the Imperial College method (Jardine et al., 2005). The following discussion of  $s_{u,rem}$  for the BDK, SBK and CK also takes into account the sleeve friction ( $f_s$ ) measured in all relevant CPTs.

Fig. 11a shows that the values of  $s_{u,rem}$  (measured mostly by fallcone) for the BDK unit exhibit significant scatter (~40–200 kPa). A single UU test for the BDK (at 10% axial strain) shows dilatant behaviour and results in  $s_{u,rem} = 45.8$  kPa which falls toward the low end of the scatter range. The  $s_{u,rem}$  for the SBK (based on limited laboratory tests) ranges between 50 and 220 kPa (Figure 11b). For both clays, the variation ranges of  $f_s$  with depth generally agree with the values of  $s_{u,rem}$  (Figures 11a and b). The correlation of  $f_s$  with  $s_{u,rem}$  is however unlikely to be universal due to various factors affecting the measurements of  $f_s$  including pore pressure, sleeve end area, sleeve roughness and degree of remoulding. The sensitivity (estimated as the ratio between intact and remoulded shear strength,  $S_t = s_u/s_{u,rem}$ ) falls between 1 and 2 for the BDK and 2–3.5 for the SBK (Table 1).

Driving piles into chalk might lead to the development of a remoulded zone along the pile shaft which can result in very low shaft resistance. This is a particular important issue at the SSOWF site due to the widespread of chalk at the site. Values of  $s_{u,rem}$  between ~200 and 300 kPa are obtained for chalk from residual ring shear, shear box and interface shear box tests. Although these values fall in the middle of the range of  $f_s$  for the CK obtained from the CPTs at the site, Lord et al. (2002) observed that the measured  $f_s$  for chalk normally exceeds the skin friction obtained in pile load tests and, hence, is unsuitable for assessing the shear resistance of driven piles into chalks. This overestimation is explained by the scale effect because the  $f_s$  represents the friction between the CPT sleeve and the intact (not remoulded)

chalk, which is amplified by an increased horizontal stress caused by lateral displacement of the block of chalk (Lord et al., 2002). To address this problem, Lord et al. (2002) recommends that a value of 20 kPa is used for the ultimate shaft resistance for small displacement driven piles into chalk unless the chalk is very intact (i.e. classified as high-density Grade A), in which case a value of 120 kPa is suggested. The value of  $f_s$  may however be applicable to an open-ended steel pile with skin friction of up to 150 kPa (Lord et al., 2002).

7. Stiffness degradation

A requirement for structures exposed to dynamic environmental loads is to keep the eigenfrequencies at a safe distance to avoid resonance with the dominating loading frequencies. This means that, for OWTs, additional requirements regarding dynamic stiffness must be taken into account due to the dynamic loads from the turbine (1P and 3P frequencies), which results in a narrow allowed frequency band (typically 0.2–0.3 Hz) for the first eigenmode of the wind turbine structure. The design of the OWT foundation is therefore sensitive to the soil stiffness. The high initial stiffnesses of soils at the SSOWF imply a potential problem of stiffness degradation (i.e. reduction of  $G$  with loading), and this needs to be properly taken into account in order to achieve reliable estimate of stiffness.

7.1. Stiffness degradation during monotonic loading

This section focuses on the degradation of secant shear modulus ( $G/G_{max}$ ) with the mobilised shear strength ( $\tau^*/\tau^*_{max}$ ). To facilitate the presentation of the results, the horizontal axes shown in Fig. 12 have been rescaled by deducting the shear stress by its initial value,  $\tau^* = \tau - \tau_{ini}$  and  $\tau^*_{max} = \tau_{max} - \tau_{ini}$  (i.e.  $\tau_{ini}$  is attained at the end of anisotropic consolidation and prior to shearing).

As can be seen from Fig. 12a, the BDK loses 50–80% of its initial stiffness once the shear strength is mobilised by 20% either under compression (i.e. positive  $\tau^*/\tau^*_{max}$ ) or extension (i.e. negative  $\tau^*/\tau^*_{max}$ ). For this clay, the variation range of  $G/G_{max}$  observed in the CAU tests is relatively consistent to that observed in the DSS tests, and both are slightly lower than the range for various clays and sands compiled in Mayne (2006) (Figure 12a). The DSS samples degrade more ‘smoothly’ than the CAU samples, which is probably due to the stronger influence of sampling disturbances on the latter compared with that on the former (Mayne, 2006). For the SBK, the ratio of  $G/G_{max}$  appears to decrease much faster in the CAU than in the DSS, which might also be attributable to the effect of sample disturbances (Figure 12b). The stiffness of the

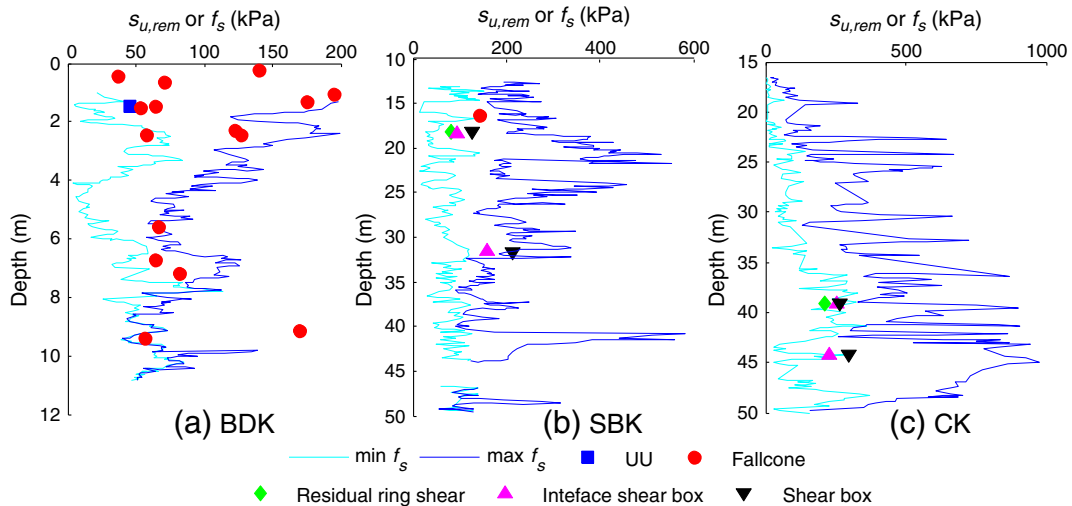
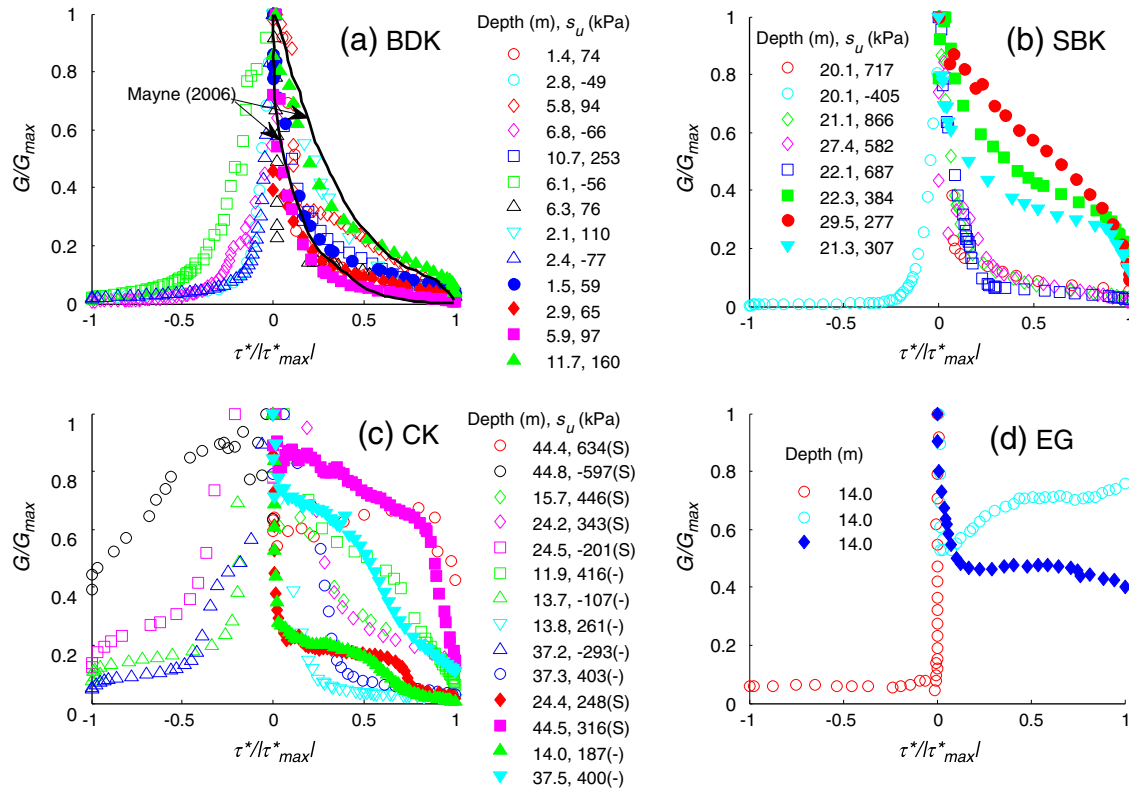


Fig. 11. Remoulded shear strength ( $s_{u,rem}$ ) and variation ranges of sleeve friction ( $f_s$ ) from all relevant CPTs.



**Fig. 12.** Degradation of secant shear modulus ( $G/G_{max}$ ) with mobilised shear strength ( $\tau^*/\tau^*_{max}$ ) in CAUC, CAUE (open symbols) and DSS tests (solid symbols), (S) = structured, (-) = structureless.

SBK degrades relatively 'smoothly' with increasing  $\tau^*/\tau^*_{max}$ , similar to the BDK. Unlike the trends observed for the BDK, SBK clays, the CK exhibits widely varying and erratic patterns of stiffness degradation (Figure 12c), which is likely due to the brittleness and variable degree of weathering of this chalk. The  $G/G_{max}$  of the EG sand reduces dramatically within very low  $\tau^*/\tau^*_{max}$  (<5%), then fluctuates around a constant value up to failure (Figure 12d). The EG samples retain <10% of its stiffness under extension and between 40 and 60% under compression.

### 7.2. Stiffness degradation during cyclic loading

Similar to monotonic loading, cyclic loading can cause significant deterioration of soil stiffness. This is a particular important issue for the SSOWF because the heavily overconsolidated state of clays, dense compaction of sand and brittleness of chalk mean that their constant subjection to cyclic loads from winds and waves can lead to considerable losses of strength. Fig. 13 shows, in a linear-log scale, that the reduction of secant cyclic shear modulus ( $G_{cy}$ ) with increasing cyclic shear strain ( $\gamma_{cy}$ ) can be very significant for the investigated range of cyclic shear stress ( $\tau_{cy}$ ) and cyclic average shear stress ( $\tau_a$ ). Note that, for most samples, the  $\gamma_{cy}$  corresponding to the first cycle (i.e. the starting point of each curve) is relatively large, and the degradation of stiffness within the small strain region is not included.

In Fig. 13, the stiffness degradation curves graphically represent the relationship  $G_{cy} = \tau_{cy}/\gamma_{cy}$  and, hence, the position of each curve is defined by  $\tau_{cy}$ . Samples subjected to  $\tau_{cy}$  of similar magnitudes therefore tend to approximately coincide which can be observed, for example, for samples (4), (6) and (7) of the BDK ( $\tau_{cy} \approx 50$  kPa), samples (1) and (4) of the EG ( $\tau_{cy} \approx 150$  kPa) or samples (1), (3) and (6) of the SBK ( $\tau_{cy} \approx 200$  kPa). An increase in  $\tau_{cy}$  shifts the curve toward the right because a larger amount of  $\gamma_{cy}$  is produced by the soil. For instance, samples (1), (7), (3) and (2) of the BDK subjected to  $\tau_{cy}$  of 31.6, 48.6, 80.1 and 103.1 kPa respectively are located increasingly toward the right on the horizontal axis (Figure 13a). These trends are applicable

to all four soil units though some exceptions can be observed. The degradation pattern of  $G_{cy}$  is consistent between the cyclic CAU results and the cyclic DSS results.

As the  $\tau_{cy}$  increases, the starting value of  $G_{cy}$  (after the 1st cycle) tends to decrease, and fewer cycles are generally required to degrade  $G_{cy}$  to a particular value (Figure 13). The reduction of  $G_{cy}$  from its starting value can be very significant in most cases. For example, compared with the value of  $G_{cy}$  after the first cycle, a decrease by at least 80% can be expected once the  $\gamma_{cy}$  reaches 3% for samples (1), (4), and (6) of the BDK; (1) and (4) of the EG and (2) and (4) of the SBK. The CK shows even more dramatic reduction in  $G_{cy}$ , in most cases, by as much as 99% at  $\gamma_{cy} = 3\%$ . The significant effect of cyclic loading on the stiffness modulus of soils at the SSOWF suggests that the value of  $G_{cy}$  used in design should be corrected according to the cyclic loading condition to which the soil has been subjected. This can be achieved using, for example, models that have been developed for stiffness degradation with cyclic loading such as Achmus et al. (2009) or Vucetic and Dobry (1988).

### 8. Soil variability and its implications on foundation design

As can be seen from the previous sections, the soil properties at the SSOWF vary quite considerably due to the geological origin and weathering condition. Table 2 shows the mean and coefficient of variation (CoV) of various soil parameters for the four soil units. The values of CoV tend to be much smaller for the index soil parameters (e.g.  $\gamma$ ,  $\gamma_{dry}$ ,  $w$ ,  $w_p$ ,  $w_L$ , and  $I_p$ ) than for those soil parameters that dictate strength and deformation (e.g.  $s_u$  and  $G_{max}$ ) (Table 2). The main reason for this is likely to be a larger natural variability of the latter compared with the former. In addition, the CoV for the index soil parameters is reduced by a considerably larger number of measurements and simpler measurement techniques (and hence entailing smaller measurement errors). The values of CoV for the index properties at the SSOWF are rather similar to the corresponding data found in the literature. For

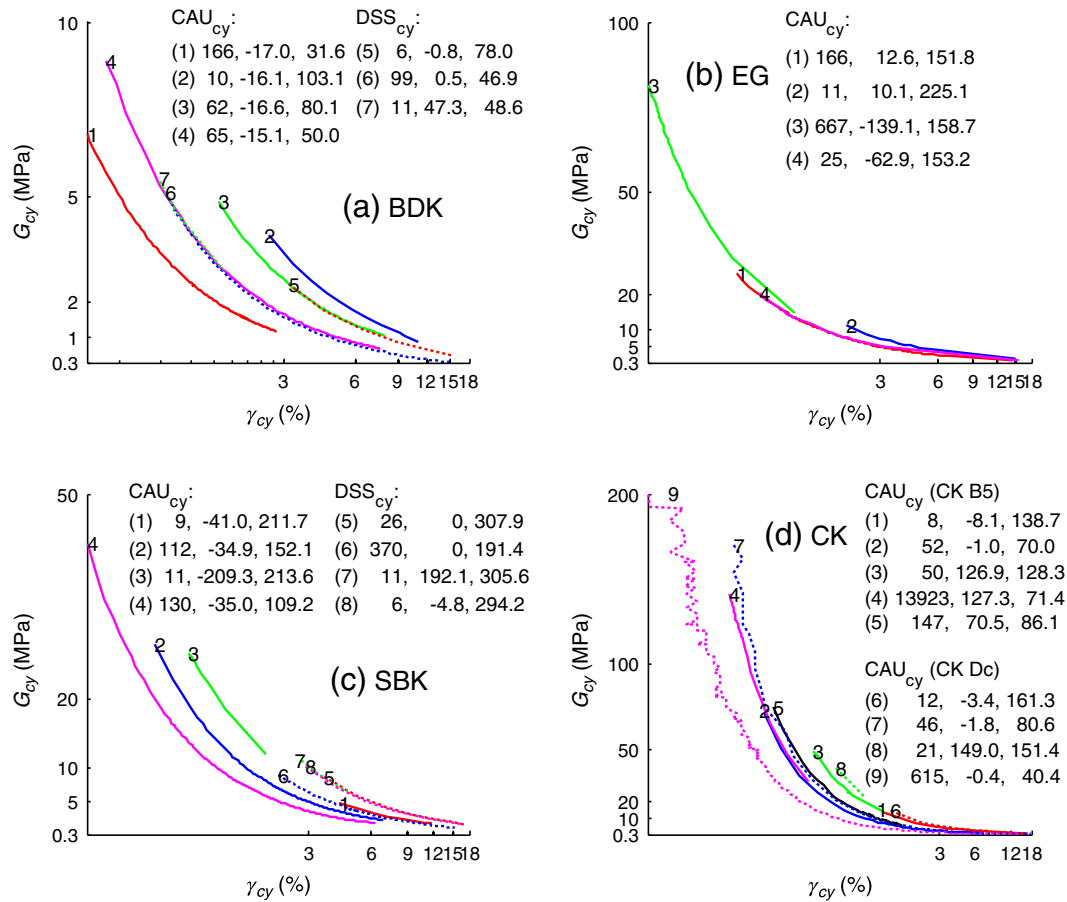


Fig. 13. Stiffness degradation with cyclic loading from CAU (continuous) and DSS (dotted) tests. Each curve is numbered with the corresponding  $(N_f, \tau_a, \tau_{cy})$  shown in the legend.

example, Phoon and Kulhawy (1999) consolidated data from various sources and reported a  $CoV = 18\%$  for  $w$ ,  $18\%$  for  $w_L$ ,  $16\%$  for  $w_p$ ,  $29\%$  for  $I_p$ ,  $9\%$  for  $\gamma$  and  $7\%$  for  $\gamma_{dry}$ . The authors also suggested that the possible variation range of  $CoV$  for each of these soil parameters and these ranges cover all the  $CoV$  values for the soils at the SSOWF. The variability

of undrained shear strength  $s_u$  at the SSOWF is larger than the corresponding values from laboratory tests reported by Phoon and Kulhawy (1999) (i.e. 49–60% compared with 22–33%), possibly due to rather limited number of samples in the current study. Conversely, the variability of friction angle  $\phi'$  is lower at the SSOWF than the typical

Table 2  
Variability of soil properties at the SSOWF.

Properties	BDK			EG			SBK			CK		
	NoS	$\mu$	CoV (%)	NoS	$\mu$	CoV (%)	NoS	$\mu$	CoV (%)	NoS	$\mu$	CoV (%)
$\gamma$ (kN/m <sup>3</sup> )	32	21.4	4	24	20.3	5	59	21.0	7	66	19.8	6
$\gamma_{dry}$ (kN/m <sup>3</sup> )	33	18.1	5	25	16.5	8	69	17.7	8	56	15.5	9
$w$ (%)	116	16.8	17	39	21.6	17	148	17.4	23	234	27.3	12
$\phi$	115	0.31	11	38	0.36	11	146	0.32	16	234	0.42	8
$w_p$ (%)	43	15.3	16	2	15.0		31	16.4	10	46	19.1	8
$w_L$ (%)	43	31.6	13	2	32.4		31	31.4	13	46	27.7	6
$I_p$ (%)	43	17.0	11	2	17.4		31	15.0	21	46	8.6	12
Clay (%)	43	31.4	23	5	17.5	60	32	34.4	32			
Clay silt (%)	31	61.0	26	17	14.2	140	23	72.1	43			
Clay silt sand (%)	31	97.5	3	17	98.7	2	32	99.2	1			
$s_{u,rem}$ (kPa)	17	95.0	51				6	137	31	5	251	12
$s_u$ (kPa)	11	123	49				31	376	53	20	296	60
$s_u^{DSS}/s_u^C$	4	0.75	25				3	0.43	5	4	0.82	25
$s_u^E/s_u^C$	3	0.67	13				1	0.48		4	0.67	33
$G_{max}$ (MPa)	4	33	61	19	114	67	29	634	37	113	1360	49
$\phi'$ (°)	9	37	8	4	46	6	5	32.9	4	11	38	6
$S_r$	15	1.4	21	2	1.8		1	1.8				
$c_v$ (m <sup>2</sup> /s)	2	$1.51 \times 10^{-7}$		1	$2.80 \times 10^{-1}$		3	$7.67 \times 10^{-6}$		4	$2.19 \times 10^{-4}$	51
$k$ (m/s)	2	$1.90 \times 10^{-10}$		1	$3.20 \times 10^{-5}$		3	$2.00 \times 10^{-9}$		4	$3.20 \times 10^{-8}$	48

NoS: number of samples.  
 $s_u$ : estimated from CAU and UU tests only.  
 $G_{max}$  for CK: ignore the depth dependency.

values in the literature (i.e. 4–8% for both sands and clays compared with 9% for sand and 9–21% for clays, silts from Phoon and Kulhawy, 1999).

The vertical correlation lengths for a few soil parameters where continuous measurements are available (e.g.  $s_u$  and OCR) are approximately 1–3 m. This is consistent with reported vertical correlation lengths for corresponding parameters from the literature (e.g. Phoon and Kulhawy, 1999 or Baecher and Christian, 2003) in which the correlation length has been derived from larger sources of data. It is not possible to reasonably estimate the horizontal correlation length (if exists) for soil parameters from the SSOWF due to limited number of measurements. If required in analysis and design, it is recommendable to use the horizontal correlation length for corresponding parameters of similar soils reported in the literature (e.g. Phoon and Kulhawy, 1999 or Baecher and Christian, 2003).

For relatively variable soil condition such as at the SSOWF, investment in soil investigation to build reliable soil models is recommended in order to reduce uncertainties and narrow down the risk. In practical design, the soil variability can be addressed following recommended practices, for example, from DNV-RP-C207 (2010). For the SSOWF site, the variability of all soil parameters is relatively large, especially for the chalk due to the existences of both weathered and intact chalks. Particular attention should be paid to the uncertainty associated rotational friction of chalk which can cause problem in designing for rotation limit.

The choice between the mean and the percentile value in design should take into account the particular problems governed by the soil parameters of interest. Strength parameters (e.g.  $s_u$  or  $s_{u,rem}$ ) play a central role in bearing capacity calculation and, hence, a conservative lower bound value (normally 5% percentile) is recommended to be used. This is particularly applicable for problems governed by a local strength value (e.g. the pile tip resistance for end-bearing capacity). Designing for installation capacity however requires an upper bound value of strength parameters which the 95% percentile is recommended. A mean value is recommended for problems involving large soil volumes where local strength variations from point to point can be assumed to average out (e.g. the pile lateral capacity, stability of large gravity foundation). Also, a mean value is also suggested for  $G_{max}$  which is an important soil parameter to wind turbine foundations. The  $G_{max}$  dictates the estimation of the eigenfrequency which should lie between 1P (rotation) and 3P (blade passing) frequencies to avoid resonance. The use of too high or too low values of  $G_{max}$  therefore can be problematic.

In designing offshore wind turbine foundations, it is important to ensure stability for the low range of strength while installation capacity for the high range of strength. However, with such large variability in shear strength as at the SSOWF, a common factor of safety that will satisfy these conditions at every location would be excessively large and becomes over-conservative at many locations. This is because the foundation will need to address the lowest and the highest shear strength values of the whole site, which are respectively lower and higher than the local lowest and highest values at many locations. Therefore, a “one-size-fits-all foundation” would be very large and safe but very costly. In addition, the foundation might become too big that it might not be possible to be installed and might not give the desired dynamic stiffness. The specific design for each location is recommended as it becomes less costly than the design for the whole site. The factor of safety is then similar at every location and should be adequate while the size of the foundation is varied with the locations.

Since the current design guideline for offshore wind turbine foundations is largely based on those from the oil and gas industry, the factor of safety is likely to be similar between offshore wind turbine foundations and foundations for oil platforms. This is provided that the oil platforms are submerged and do not support human activity and the wind turbine foundation is designed for each specific location. If the wind turbine foundations are designed following the guideline for the oil and gas facilities which are required to support human activities on board, then their factor of safety would probably be over-conservative because the

wind turbines have a different safety class (as they do not pose threat to human life upon failure). In cases where a one-site-fits-all solution is used in highly variable soils, the FoS for an offshore wind farm is likely to be much larger than for oil facilities in similar soils due to much larger number of measurements.

## 9. Conclusions

The four main soil units at the Sheringham Shoal offshore wind farm in the North Sea (Bolders Bank Formation, BDK; Egmond Ground Formation, EG; Swarte Bank Formation, SBK and Chalk Unit, CK) have been characterised in this study in the context of designing foundations for offshore wind turbines to provide a realistic case study for research and practice. The characterisation shows that the soil behaviour at this site is dictated by the marine glacial origin with repeated glaciation cycles. Particularly, the BDK and SBK clays are heavily overconsolidated with relatively low water content, low plasticity, medium to high rate of consolidation and low permeability. The EG sand is densely compacted with high relative density, high rate of consolidation and high permeability. The CK chalk shows typical weak and brittle rock behaviour with very low plasticity, high consolidation rate and low permeability, though the properties of the CK tend to vary quite significantly with depth due to its variable weathering state.

The undrained shear strengths of the BDK, SBK and CK are, on average, quite high but show large differences between the upper and lower bound strengths. The drained shear strength of the EG is also high. The wide differences in the bound shear strength values pose a challenge in the design of the foundation dimensions which are favourably large to be stable at the lower bound strength but small to be installable at the upper bound strength. Therefore, a specific design strategy is recommended at this site to deal with the considerable soil variability. This means that the foundations vary in sizes depending on the soil properties at each turbine location. The remoulded shear strengths of the BDK and SBK are from one to three times lower than the intact shear strength. The remoulded shear strength value must be used with extreme caution for locations with a substantially thick chalk layer due to the overestimation of pile shaft resistance by the CPT sleeve friction.

All four soil units exhibit high to very high small strain stiffness which increases with depth and tends to be larger than the stiffness of some well-characterised soils in nearby areas. The degradation of stiffness modulus with monotonic or cyclic loads is identified as a particularly important issue for the Sheringham Shoal wind farm because of the high initial stiffnesses. In the case of monotonic loading, analyses of the secant shear moduli measured in triaxial and direct simple shear tests suggest that the reduction of stiffness with the mobilised shear strength can be significant for all four soils and the pattern of degradation varies considerably among them. The cyclic shear stiffness of these soils also degrades substantially with cyclic loading. This highlights a concern for the Sheringham Shoal or similar sites because of the constant exposure of the wind turbine foundations to cyclic loads from winds and waves.

## Acknowledgement

The authors wish to gratefully acknowledge Statoil AS (Norway) and Statkraft AS (Norway) for providing access and permission to publish the data from the Sheringham Shoal offshore wind farm. The authors express gratitude to Statoil AS and DNV (Norway) for their eager contribution and financial support to this project. Prof. Steinar Nordal (NTNU, Norway) is sincerely thanked for reviewing the manuscript. Gardline Geosciences Ltd (UK) is acknowledged for performing the borehole sampling and establishing a ground model combining geophysical and geotechnical data. GEO (Danish Geotechnical Institute) is acknowledged for conducting the CPT measurements. The NGI (Norwegian Geotechnical Institute) is thanked for performing the the majority of

laboratory experiments and preparing the geotechnical interpretation report (under contract with Gardline).

## References

- Achmus, M., Kuo, Y.-S., Rahman, K.A., 2009. Behavior of monopile foundations under cyclic lateral load. *Comput. Geotech.* 36, 725–735.
- Andresen, A., Berre, T., Kleven, A., Lunne, T., 1979. Procedures used to obtain soil parameters for foundation engineering in the North Sea. *Mar. Geotechnol.* 3 (3), 201–266.
- Baecher, G.B., Christian, J.T., 2003. *Reliability and Statistics in Geotechnical Engineering*. Wiley, Chichester, United Kingdom.
- Baldi, G., Bellotti, R., Ghionna, V., Jamiolkowski, M., Pasqualini, E., 1986. Interpretation of CPTs and CPTUs; 2nd part: drained penetration of sands. *Proceedings of the Fourth International Geotechnical Seminar*, Singapore, pp. 143–156.
- Bell, F.G., 2002. The geotechnical properties of some till deposits occurring along the coastal areas of eastern England. *Eng. Geol.* 63 (1–2), 49–68.
- Bell, F.G., Culshaw, M.G., Cripps, J.C., 1999. A review of selected engineering geological characteristics of English Chalk. *Eng. Geol.* 54 (3–4), 237–269.
- Birchall, R., 2012. The need to integrate geophysical with geotechnical data to aid pile design and installation: a case study of the Sheringham Shoal offshore wind farm. *Proceedings of the Seventh International Conference in Offshore Site Investigation and Geotechnics*, London, UK, 12–14 September 2012. Society for Underwater Technology (SUT).
- Bjerrum, L., 1973. Geotechnical problems involved in foundations of structures in the North Sea. *Geotechnique* 23 (3), 319–358.
- Byrne, B.W., Houlsby, G.T., 2006. Assessing novel foundation options for offshore wind turbines. *World Maritime Technology Conference*, London, UK.
- Cameron, T.D.J., Crosby, A., Balson, P.S., Jeffery, D.H., Lott, G.K., Bulat, J., Harrison, D.J., 1992. *United Kingdom Offshore Regional Report: The Geology of the Southern North Sea*. Clayton, C.R.L., 2011. Stiffness at small strain: research and practice. *Geotechnique* 61 (1), 5–37.
- Cripps, J.C., Taylor, R.K., 1986. Engineering characteristics of British over-consolidated clays and mudrocks I. Tertiary deposits. *Eng. Geol.* 22 (4), 349–376.
- Cripps, J.C., Taylor, R.K., 1987. Engineering characteristics of British over-consolidated clays and mudrocks, II. Mesozoic deposits. *Eng. Geol.* 23 (3–4), 213–253.
- DNV, 1992. DNV No 30.4 – Classification Notes – Foundations. Det Norske Veritas, Oslo, Norway.
- DNV, 2010. DNV-RP-C207 Recommended Practice – Statistical Representation of Soil Data. Det Norske Veritas, Oslo, Norway.
- DNV, 2011. Design of Offshore Wind Turbine Structures: DNV-OS-J101 (Sep, 2011). Det Norske Veritas, Oslo, Norway.
- Eide, O., Andersen, K.H., 1984. Foundation engineering for gravity structures in the northern North Sea. *Proceedings of the International Conference on Case Histories in Geotechnical Engineering*, St Louis, Missouri, pp. 1627–1678.
- Elhakim, A.F., 2005. Evaluation of shallow foundation displacements using soil small strain stiffness. (PhD) Georgia Institute of Technology, Atlanta, Georgia, US.
- Firouziandbandpey, S., Ibsen, L.B., Andersen, L.V., 2012. CPTu-based geotechnical site assessment for offshore wind turbines – a case study from the Aarhus site in Denmark. *Proceedings of the Twenty-second (2012) International Offshore and Polar Engineering Conference*, Rhodes, Greece June 17–22, 2012. ISOPE.
- Gasparre, A., 2005. Advanced laboratory characterization of London clay. (PhD) Imperial College London.
- GeoVision, 1994. Suspension P–S velocity logging method. [online]. Available from [www.geovision.com](http://www.geovision.com) (cited 15th Aug 2012).
- Hamre, L., Khankandi, S.F., Strøm, P.J., Athanasiu, C., 2010. Lateral behaviour of large diameter monopiles at Sheringham Shoal Wind Farm. *Proceedings of the 2nd International Symposium on Frontiers in Offshore Geotechnics*, Perth, Australia. Taylor & Francis Group, London, pp. 575–580.
- Houlsby, G.T., Byrne, B.W., Martin, C.M., 2001. *Novel Foundations for Offshore Wind Farms*. EPSRC, Department of Engineering Science, Oxford University, United Kingdom, p. 9.
- Jardine, R., Overy, R., Chow, F., 1998. Axial capacity of offshore piles in dense North Sea sands. *J. Geotech. Geoenviron. Eng.* 124 (2), 171–179.
- Jardine, R., Chow, F., Overy, R., Standing, J., 2005. *ICP Design Methods for Driven Piles in Sands and Clays*. Thomas Telford Publishing, London.
- C.C.Ladd, C.C., 1991. Stability evaluation during staged construction: Terzaghi lecture]. *Geotech. Eng. ASCE* 117 (4), 540–615.
- Lehane, B.M., Jardine, R.J., 1994. Displacement pile behaviour in glacial clay. *Can. Geotech. J.* 31 (1), 79–90.
- Long, M., Donohue, S., 2010. Characterization of Norwegian marine clays with combined shear wave velocity and piezocone cone penetration test (CPTU) data. *Can. Geotech. J.* 47 (7), 709–718.
- Long, M., Menkiti, C.O., 2007. Geotechnical properties of Dublin Boulder Clay. *Geotechnique* 57 (7), 595–611.
- Lord, J.A., Clayton, C.R.L., Mortimore, R.N., 2002. *Engineering in Chalk*. CIRIA Report C574. Construction Industry Research and Information Association (CIRIA) (London).
- Lunne, T., Robertson, P.K., Powell, J.J.M., 1997. *Cone Penetration Testing in Geotechnical Practice*. Blackie Academic & Professional, London.
- T.Lunne, T., M.Long, M., M.Uzielli, M., 2006. Characterisation and engineering properties of Troll ClayIn: Phoon, K.K., Hight, D.W., Leroueil, S., Tan, T.S. (Eds.), *Characterisation and Engineering Properties of Natural Soils: Proceedings of the Second International Workshop on Characterisation and Engineering Properties of Natural Soils*. Taylor & Francis, Singapore.
- Mayne, P., 2006. In-situ test calibrations for evaluating soil parameters. *Characterisation and Engineering Properties of Natural Soils*. Taylor & Francis.
- Mayne, P.W., Kulhawy, F.H., 1982. K<sub>0</sub>–OCR relationships in soil. *J. Geotech. Eng.* 108 (GT6), 851–872.
- Phoon, K., Kulhawy, F., 1999. Characterization of geotechnical variability. *Can. Geotech. J.* (36), 612–624.
- Rambøll, 2011. *Geotechnical properties for Cretaceous Chalk (GRD 00.1-001-E)*. Rambøll Arup Joint Venture & Rambøll Danmark A/S, Copenhagen, Denmark.
- M.Saue, M., V.Meyer, V., 2009. *Geotechnical Report: Sheringham Shoal Wind Farm Soil Investigation (20081313-1)*. Norwegian Geotechnical Institute (NGI), Oslo, Norway.
- M.J.Siegerta, M.J., J.A.Dowdeswell, J.A., 2004. Numerical reconstructions of the Eurasian Ice Sheet and climate during the Late Weichselian. *Quat. Sci. Rev.* 23, 1273–1283.
- Smith, G.J., Rosenbaum, M.S., 1993. Recent underground investigations of abandoned chalk mine workings beneath Norwich City, Norfolk. *Eng. Geol.* 36 (1–2), 67–78.
- Tanaka, H., Locat, J., Shibuya, S., Soon, T.T., Shiwakoti, D.R., 2001. Characterization of Singapore, Bangkok, and Ariake clays. *Can. Geotech. J.* 38 (2), 378–400.
- Vucetic, M., Dobry, R., 1988. Degradation of marine clays under cyclic loading. *J. Geotech. Eng.* 2 (114), 133–149.
- Vucetic, M., Dobry, R., 1991. Effect of soil plasticity on cyclic response. *J. Geotech. Eng. ASCE* 117 (1), 89–107.
- Wroth, C.P., 1984. The interpretation of in-situ soil tests. *Geotechnique* 34 (4), 449–489.